IOP Publishing Plasma Sources Science and Technology

Plasma Sources Sci. Technol. **23** (2014) 045014 (7pp) doi:10.1088/0963-0252/23/4/045014

Temperature gradients due to adiabatic plasma expansion in a magnetic nozzle

J P Sheehan[1], B W Longmier[1], E A Bering[2], C S Olsen[3], J P Squire[3], M G Ballenger[4], M D Carter[3], L D Cassady[3], F R Chang Díaz[3], T W Glover[3] and A V Ilin[3]

[1] University of Michigan, 1320 Beal Ave, Ann Arbor, MI 48109
[2] University of Houston, 617 Science & Research Bldg 1, Houston, TX 77004, USA
[3] Ad Astra Rocket Company, 141 W. Bay Area Blvd, Webster, TX 77598, USA
[4] Space Exploration Technologies, 1 Rocket Rd., McGregor, TX 77598, USA

E-mail: sheehanj@umich.edu

Received 2 February 2014, revised 18 April 2014
Accepted for publication 13 June 2014
Published 7 July 2014

Abstract

A mechanism for ambipolar ion acceleration in a magnetic nozzle is proposed. The plasma is adiabatic (i.e., does not exchange energy with its surroundings) in the diverging section of a magnetic nozzle so any energy lost by the electrons must be transferred to the ions via the electric field. Fluid theory indicates that the change in plasma potential is proportional to the change in average electron energy. These predictions were compared to measurements in the VX-200 experiment which has conditions conducive to ambipolar ion acceleration. A planar Langmuir probe was used to measure the plasma potential, electron density, and electron temperature for a range of mass flow rates and power levels. Axial profiles of those parameters were also measured, showing consistency with the adiabatic ambipolar fluid theory.

Keywords: magnetic nozzle, adiabatic, VASIMR, electric propulsion, helicon

(Some figures may appear in colour only in the online journal)

1. Introduction

In recent years there has been significant interest in helicon discharges in expanding magnetic fields for applications such as spacecraft propulsion [1] and plasma processing [2] as well as for studies in basic plasma science [3–6]. Helicon discharges are used to efficiently produce plasma [7] while the diverging magnetic field produces an ion beam which has the potential for producing thrust for space applications or etching in processing applications [2, 8]. This article describes the acceleration mechanism observed in a helicon source and magnetic nozzle for use in an electromagnetic propulsion device.

Typical experiments involve a helicon antenna surrounding a non-conductive tube in which the plasma is created (called the source chamber) which is attached to a larger diameter conducting chamber (called the expansion chamber). The magnetic field expands from the source chamber into the expansion chamber with a corresponding drop in field strength, a scheme which serves to accelerate ions. Current-free double layers (CFDLs), narrow (10 s of Debye lengths), adjacent regions of equal and opposite space-charge, are commonly observed as the accelerating mechanism in laboratory experiments [9–11], which is relevant for processing, but it is unknown whether that mechanism would apply to a helicon thruster in space. Ambipolar ion acceleration has been considered as an alternative mechanism that may be more relevant to the space environment where collisions with neutrals are far less significant [12, 13]. This paper shows that experimental data are consistent with two-fluid theory predictions of the behavior of plasma parameters for ambipolar ion acceleration in an adiabatic plasma.

Double layers formed in helicon generated plasmas with expanding magnetic fields are current free because there are no plasma facing electrodes in the source region through which to draw a current. A variety of theories exist about how and why CFDLs form in expanding magnetic fields. It has been observed that double layers form when the ion-neutral mean free path is comparable to or larger than the density gradient scale length or magnetic field gradient scale length [14]. One formulation relies on electrons born

downstream that accelerate back up the potential structure [15]. Another possibility is two electron populations with different temperatures can enforce the current balance [16, 17]. A rather different theory suggests that double layers in these devices are simply sheaths that exist in free space to enforce the current-free condition [18]. No consensus has yet been reached as to why CFDLs form.

Recently, probe measurements were made in the VX-200 experiment, a helicon generated plasma with a magnetic nozzle and an ion cyclotron heater (ICH), though the ICH was unused in those experiments [13]. An ion accelerating potential was observed but, surprisingly, it extended of 10 000 s of Debye lengths, rather than 10 s, indicating that this structure was not a double layer. Instead, ambipolar electric fields established the potential structure and accelerated the ions. This phenomenon is explored in greater detail in this article.

2. Ion acceleration mechanisms

2.1. Current-free double layers

One mechanism for ion acceleration in a diverging magnetic field is that a CFDL is established near the plane separating the source chamber from the expansion chamber. The space-charge regions of the double layer establish a potential drop of 1 or 10 s of T_e/e's for weak and strong double layers, respectively, where T_e is the electron temperature in eV, in a region of 10 s of Debye lengths. Although double layers can easily be formed when a plasma is carrying current, CFDLs form even when there is no net current across the double layer [16].

In a double layer four species can be considered: free ions and trapped electrons originating in the source chamber and trapped ions and free electrons originating in the expansion chamber. Free species can pass across the double layer, for instance ions accelerating through a potential drop or a beam of electrons with energy larger than the double layer potential. Trapped species are unable to cross the double layer and can be low energy ions produced downstream or low energy electrons upstream. Downstream refers to the low potential side of the double layer and upstream to the high potential side because most of the plasma is generated on the high potential side.

2.2. Rarefaction wave theory

A kinetic theory has been proposed to describe ambipolar ion acceleration [12, 19]. The full velocity distribution function of the electrons was considered and it was assumed that the ions were cold and followed the fluid equations. The electrons were strongly magnetized and tied to the field lines. The plasma was generated upstream of the throat and allowed to stream through the magnetic nozzle. It was assumed that rarefaction waves far downstream in the low magnetic field region created large potential barriers that reflected most of the electrons, maintaining current balance. The solution consisted of a steady-state part upstream of the rarefaction waves and a time-dependent part where the waves were located. The motivation for assuming the presence of these waves came from magnetohydrodynamic simulations [20]. The electrons

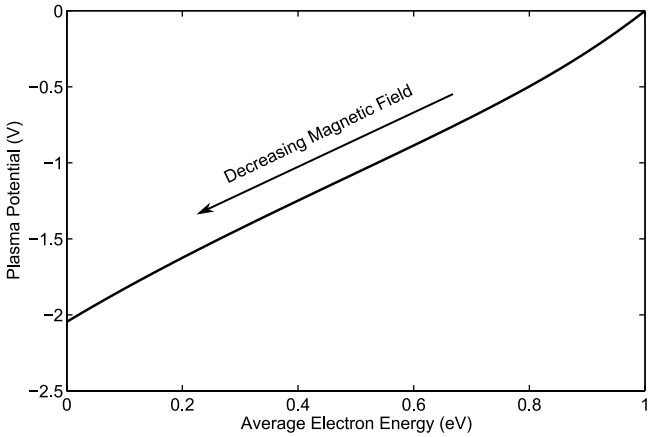

Figure 1. Rarefaction wave theory of the plasma potential versus average electron energy in the downstream region of the magnetic nozzle.

were assumed to lose energy in these reflections and become trapped downstream, resulting in a decreasing average energy as a function of distance from the throat. The electron energy distribution function in the steady-state region had a depleted high energy tail. The rarefaction wave in the region of small magnetic field where the solution was time dependent further accelerated the ions. The ion velocity at the end of the steady state region was $\sim 2c_s$, where c_s is the sound speed in the throat, and $\sim 7c_s$ at the end of the time-dependent region. The ion kinetic energy after the rarefaction wave is larger than total energy upstream of the nozzle so the plasma in this construction must draw energy from its surroundings and cannot be adiabatic.

This formulation can be used to solve for the plasma potential (ϕ, where $\phi = 0$ at the throat), electron density (n_e), and average electron energy ($\langle\epsilon\rangle$) in the steady-state region assuming that the inlet plasma is Maxwellian [19]. The values of those three parameters drop in the downstream region as the magnetic field strength decreases, consistent with experimental observations [13]. The plasma potential is graphed versus average electron energy in figure 1 for an upstream electron temperature of 1 eV. The plasma potential is approximately linearly related to average electron energy with the relationship $\frac{\partial(e\phi)}{\partial s} = 1.92\frac{\partial(\langle\epsilon\rangle)}{\partial s}$ (see figure 1), where s is the field aligned position vector. The plasma potential versus electron density is shown in figure 2. Figures 1 and 2 provide relationships between measurable parameters and are useful in comparing the theory's predictions to experimental data. Far downstream where the magnetic field is negligible, the rarefaction wave continues to accelerate the ions. The majority of the energy is transferred to the ions in the rarefaction wave, though that phenomenon has not been observed in experiments.

2.3. Adiabatic expansion

A new mechanism is presented here to describe ambipolar ion acceleration and will be referred to as the adiabatic theory. Consider a one dimensional plasma with magnetized electrons and ions in a magnetic nozzle. Assume that at any given point the electrons are Maxwellian, though the temperature

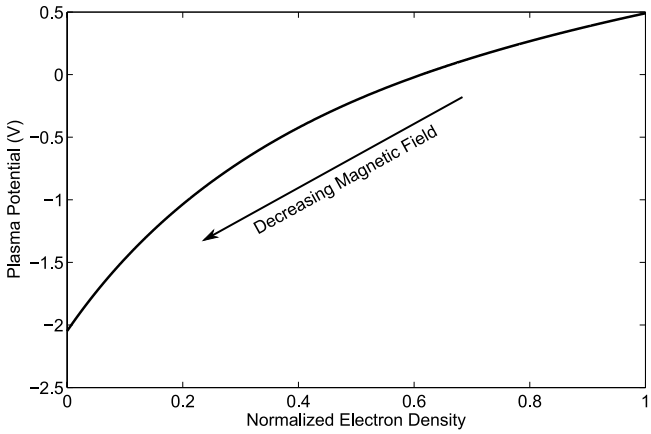

Figure 2. Rarefaction wave theory of the plasma potential versus electron density normalized to inlet electron density in the downstream region of the magnetic nozzle.

is a function of position. This assumption is consistent with experimental observations [13], though rather unexpected. Typically conduction along magnetic field lines is high, resulting in isothermal electrons. Enhanced collisionality, for instance, from ion acoustic instabilities, can both reduce the conduction and thermalize the electron distribution. With these assumptions, the electron momentum equation reduces to a balance between the pressure and potential gradient

$$\frac{\partial p_e}{\partial s} = n_e \frac{\partial (e\phi)}{\partial s} \tag{1}$$

where p_e is the electron pressure and the derivatives are with respect to the field aligned position vector enabling capture of the magnetic field expansion of a magnetic nozzle [21]. If the ions and electrons exchange energy with each other via the electric field but do not exchange energy with their surroundings (i.e., energy losses to inelastic collisions and radiation are small), the plasma as a whole (ions and electrons together) can be said to be adiabatic. The plasma pressure, dominated by the electron pressure, is related to density by the adiabatic equation of state

$$p_e = C n_e^{\gamma} \tag{2}$$

where C is a constant, $\gamma = (N+2)/N$ is the ratio of specific heats, and N is the number of degrees of freedom. If the electrons are Maxwellian (as seen in experiments), then the pressure can also be expressed as

$$p_e = n_e T_e \tag{3}$$

by taking the correct moment of the distribution function. Using equations (1)–(3), the relationship between density and potential is

$$\frac{\partial (e\phi)}{\partial s} = \frac{C\gamma}{\gamma - 1} \frac{\partial \left(n_e^{\gamma - 1} \right)}{\partial s}. \tag{4}$$

The change in plasma potential can be related to the change in electron temperature.

$$\frac{\partial (e\phi)}{\partial s} = \frac{\gamma}{\gamma - 1} \frac{\partial T_e}{\partial s} \tag{5}$$

If the plasma streams out of the magnetic nozzle with no boundary or neutral interactions it is adiabatic with 2 degrees of freedom. The average electron energy of a Maxwellian distribution is $\langle \epsilon \rangle = \frac{N}{2} T_e$, so equations (4) and (5) can be expressed as

$$\frac{\partial (e\phi)}{\partial s} = 2C \frac{\partial n_e}{\partial s} \tag{6}$$

and

$$\frac{\partial (e\phi)}{\partial s} = 2 \frac{\partial T_e}{\partial s} = 2 \frac{\partial (\langle \epsilon \rangle)}{\partial s}. \tag{7}$$

The electron energy decreases as the plasma potential decreases. The ratio of change in potential to change in energy is equal to the ratio of specific heats.

$$\frac{\Delta e\phi}{\Delta \langle \epsilon \rangle} = \frac{N+2}{N} = \gamma \tag{8}$$

The ratio decreases for a larger number of degrees of freedom.

As the ions get accelerated through the diverging section of the magnetic nozzle their density decreases which the electrons must match to maintain quasineutrality. But the electron pressure gradient must continue to balance the electric field which requires the electron temperature to decrease as well. The mechanism for the electron energy loss may be an ion-acoustic instability which would exchange energy between the ions and electrons but not affect the adiabaticity of the plasma as a whole, [22, 23] but such an analysis is beyond the scope of this work.

Equation (7) indicates behavior nearly identical to the rarefaction wave theory (see figure 1), with a linear relationship between average electron energy and potential. Both theories suggest that the electron temperature must drop by ~0.5 eV for a corresponding 1 V potential drop. The conclusions are the same even though in the rarefaction wave theory the plasma is not adiabatic since the electrons lose energy in reflections off of the rarefaction wave. Additionally, the adiabatic theory is a local theory, relying on some effective collisions to Maxwellianize the velocity distribution at every point while the rarefaction wave theory is a nonlocal theory accounting for distribution functions with depleted tails. This relationship between change in temperature and change in potential is crucial because the scaling of that relationship dictates the maximum energy impartable to ions moving through a magnetic nozzle, a key parameter for both plasma processing and electric propulsion. The behavior of the potential versus density, however, is different between the two theories, with the rarefaction wave theory indicating a negative second derivative of the function $\phi(n_e)$ (see figure 2) and the adiabatic theory indicating a linear relationship.

3. Experimental setup

Experiments on ion acceleration in a magnetic nozzle were performed in the Variable Specific Impulse Magnetoplasma Rocket (VASIMR®) VX-200 experiment, a prototype electrodeless plasma propulsion device for spacecraft [13, 24, 25]. The VX-200 device used a helicon antenna to ionize the propellant gas to a 95% ionization fraction and

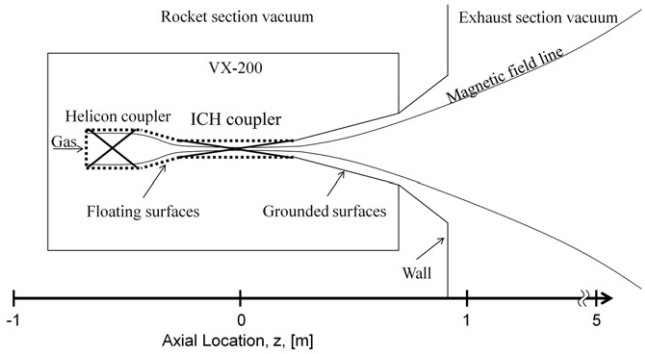

Figure 3. A schematic diagram of the experimental setup of the VX-200 device.

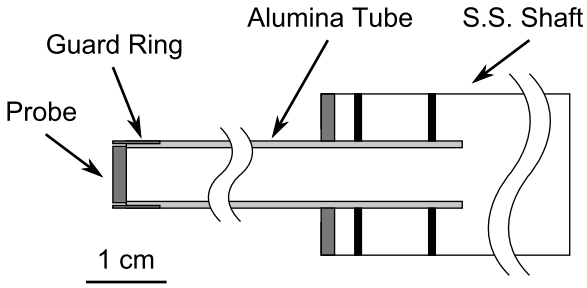

Figure 4. A schematic diagram of the planar Langmuir probe.

heat the electrons, and an ICH antenna to heat the ions. Electromagnets generated a converging/diverging magnetic nozzle to accelerate the plasma out of the device and generate thrust. For these experiments the ICH was not used. A schematic of the experiment is shown in figure 3. The magnetic field lines converge after the helicon coupler, creating a maximum in the magnetic field inside of the ICH region. This maximum is the throat and the point of reference for the measurements.

Up to 30 kW of RF power near 6.78 MHz was coupled into the plasma via the helicon antenna with a coupling efficiency of 95% [26]. The working gas was argon with mass flow rates between 50 and 140 mg s^{-1}. The electromagnets generated a maximum magnetic field of 20 kG in the throat of the magnetic nozzle (located at $z = 0$ in figure 3). All of the plasma facing components of the VX-200 were electrically floating, though the vacuum chamber was grounded. The vacuum chamber was 4.2 m in diameter and 10 m long. Cryogenic pumps provided a high pumping speed of 1.85×10^5 L s^{-1} on argon which could establish a base pressure of 10^{-9} Torr. More details about the vacuum chamber can be found in [13]. During operation the neutral pressure in the chamber was up to 10^{-4} Torr, depending linearly on the mass flow rate. The background neutral pressure resulted in a maximum charge exchange collision mean free path of ~1 m which was longer than the electric field gradient scale length. Therefore, neutral collisions were assumed to be insignificant.

The plasma was diagnosed using a planar Langmuir probe, schematically depicted in figure 4. A stainless steel tube supported an alumina tube on which the probe was mounted, keeping the probe far enough away from the grounded stainless steel tube to prevent its influence on the measurements. The probe itself was a 6.35 mm diameter tungsten disk. A 7.5 mm outer diameter, 8.0 mm long tube called the guard ring fit around the tip of the probe as indicated in figure 4. The guard ring was electrically insulated from the probe and allowed to float, which reduced sheath expansion effects that can introduce errors in probe measurements [27]. The Langmuir probe was mounted on a two dimensional motion control table which could move the probe axially and radially in the horizontal plane.

Langmuir probe current–voltage (I–V) traces were obtained by sweeping the bias on the probe from −40 to 40 V with a sweep rate of 80 Hz and a sampling rate of 40 kHz, which captured all features of the I–V trace from ion saturation current to electron saturation current. The traces were obtained in the diverging portion of the magnetic nozzle to within 50 cm of the throat. Further into the nozzle the energy densities were too high to safely operate the Langmuir probe. Because the probe measurements were made almost 1 m away from the helicon antenna, RF fluctuations were minimal, introducing 0.2 V and 0.1 eV errors to the plasma potential and electron temperature, respectively. These variations were approximately 1% of the measured values, an acceptable uncertainty, so no RF compensation scheme was used. The plane of the probe was oriented normal to the magnetic field and the probe was much larger than the electron gyroradius, so the magnetic field effects were assumed to be small.

4. Measurements

Plasma potential, electron temperature, and electron density were extracted from the I–V traces. Electron temperature was calculated from the slope of the semilog plot of the electron current to the planar Langmuir probe. Because the Langmuir probe was oriented normal to the magnetic field, the measured temperature was the parallel temperature. The knee of the I–V trace was used to identify the plasma potential and the electron saturation current which was used with temperature to calculate the density [28]. Measurements were made on the axis of the device, 50 cm downstream of the nozzle throat in the diverging region, with mass flow rates ranging from 50 to 140 mg s^{-1} and helicon powers ranging from 14 to 30 kW. Figure 5 shows how the plasma parameters vary with mass flow rate and RF power. As the RF power was increased, the plasma density increased until the plasma was approximately fully ionized. Beyond that point, additional power increased the electron temperature, which resulted in a higher plasma potential as well. Higher mass flow rates provided more neutral gas and thus a higher density when the plasma was fully ionized but also a lower electron temperature and plasma potential.

Axial profiles of the parameters were measured between 50 and 500 cm downstream of the magnetic nozzle throat. These values are shown in figure 6 for mass flow rates of 50 and 140 mg s^{-1} and helicon power of 30 kW. The uncertainties in the plasma density, potential, and electron temperature were ±10%, ±0.5 V, and ±0.5 eV, respectively, over the whole range of axial positions. The plasma density, potential, and temperature all decayed as the magnetic field strength decreased downstream of the throat of the magnetic nozzle.

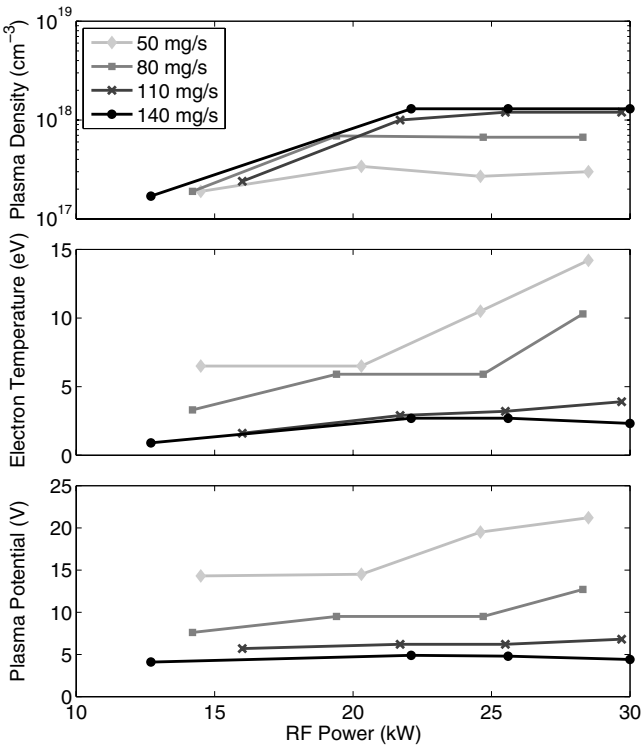

Figure 5. Key plasma parameters versus mass flow rate and power flow density measured 50 cm downstream of the nozzle throat.

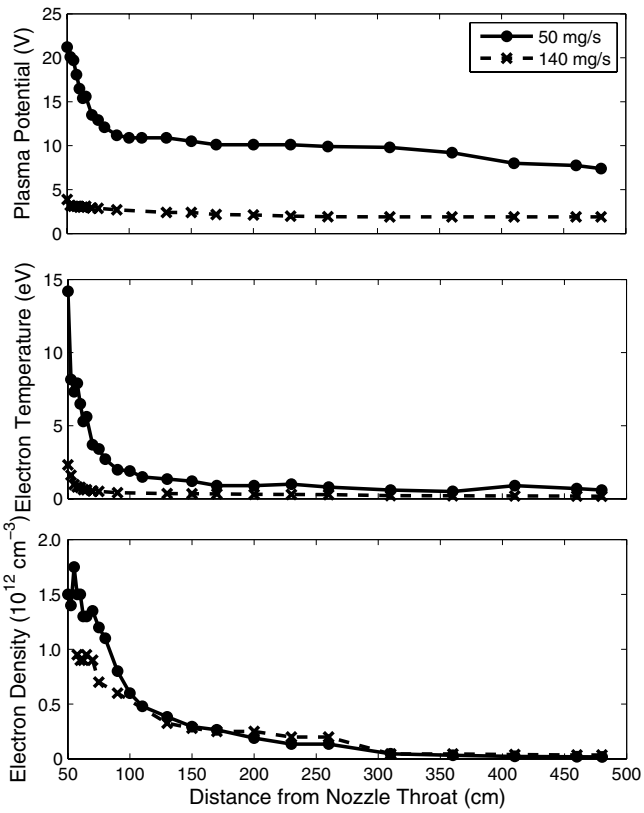

Figure 6. Plasma potential, electron temperature, and electron density as a function of distance downstream of the throat of the magnetic nozzle.

The Boltzmann relation was not applicable for this experiment because of the electron temperature gradient. Additionally, the potential drop occurs on the order of 100 cm, which is on the order of $10^5\lambda_D$, so the structure is not a double layer but ambipolar ion acceleration.

5. Discussion

Insight can be gained by comparing the change in electron temperature to the change in plasma potential for the 50 mg s^{-1} flow rate data set (see figure 7). The majority of data points fit a linear trend quite well and can be described by the equation

$$\frac{\partial(e\phi)}{\partial s} = 1.17\frac{\partial T_{e,\parallel}}{\partial s}. \quad (9)$$

Deviation at the higher temperatures close to the magnetic nozzle was due to uncertainty in the measurements at very high densities. Far downstream where the temperature was low the data do not fit the linear trend either. This may have been due to detachment, effects of the vacuum chamber walls, or that the vacuum chamber stopped the plasma from continuing to expand. A larger value of the ratio of change in potential to change in temperature is desirable because there is more ion acceleration for a given change in electron temperature.

Both the adiabatic theory and rarefaction wave theory predict that the average energy (or temperature) is linearly related to the plasma potential with a ratio of change in potential to change in average energy of 2. The measurements of that ratio were lower because only the parallel electron energy was measured. The Langmuir probe was oriented normal to the magnetic field, so perpendicular energy was not accounted for. The perpendicular electron temperature would be expected to contribute energy on the same order as the parallel energy. If the total average electron energy was twice the measured temperature in one of the two degrees of freedom, the theory and data would match well. Discrepancy between the experiment and theory could also have resulted from energy loss mechanisms such as turbulence, collisions, and radiative losses. Alternatively, the effective number of degrees of freedom could be larger than 2, possibly due to collisionality which could detach the plasma from the magnetic

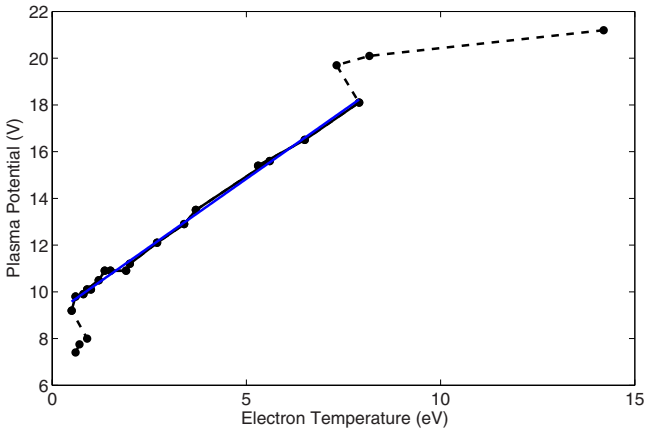

Figure 7. Plasma potential versus electron temperature in the magnetic nozzle. The blue line is a linear fit and the dashed lines connect data points that were not included in the fitted data set.

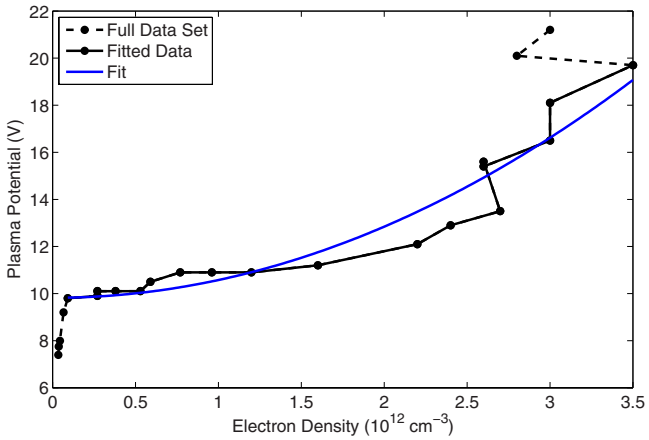

Figure 8. Plasma potential versus electron density in the magnetic nozzle. The blue line is a $\phi \propto n^2$ fit and the dashed lines connect data points that were not included in the fitted data set.

field lines. Although the electron-ion and electron-neutral collisions lengths (>1 m) were greater than the magnetic field gradient length, instability enhanced collisions may result in a higher collisionality, though that topic is beyond the scope of this work.

The relationship between the plasma potential and electron density is a distinguishing factor between the rarefaction wave and adiabatic theories. The rarefaction wave theory predicts a relationship with a negative second derivative (see figure 2), meaning the plasma potential drops the most when the electron density is low. By contrast, the adiabatic theory with 2 degrees of freedom predicts a linear relationship (see equation (6)). The data shown in figure 8 confound both predictions and show a positive second derivative. The scatter in the data is too large to reliably fit a power law with an unknown exponent, but the trend is consistent with such behavior as the $\phi \propto n^2$ shows. For the same reasons as in the previous figure, the extreme points were neglected in the fit. This behavior is consistent with the adiabatic theory predictions if instabilities increase the collisionality and effective degrees of freedom.

The mechanism for ion acceleration is critical when developing models for plasma thrusters with magnetic nozzles. The exit velocity of the ions determines the specific impulse and thrust. In an isothermal CFDL the electric fields are determined by density gradients and are not limited by the electron temperature. In the rarefaction wave theory the majority of the ion speed is due to acceleration by the rarefaction wave in the low field region. The adiabatic theory proposed here suggests that the ion acceleration is limited by the electron temperature and that there is no rarefaction wave to give the ions additional velocity after the magnetic nozzle. This theory suggests that maximizing the electron temperature is the key factor in improving thruster performance. Further experiments need to be done to verify this prediction, as both the magnitude and mechanism of thrust production are still open questions [5, 29].

6. Conclusion

A theory of adiabatic plasma expansion driven ambipolar ion acceleration was presented, predicting a linear relationship between the average electron energy and the plasma potential with a 2 volt decrease in plasma potential for every electron volt decrease in average electron energy. The electrons were assumed to rethermalize to a Maxwellian on shorter length scales than the electric field, resulting in a Maxwellian distribution at every position but with a varying temperature. This rethermalization is consistent with measurements but the mechanism is still unknown. The temperature decreases with potential to balance the electron pressure with the electric field.

Measurements of plasma potential, electron temperature, and electron density were made in a high power helicon thruster using a planar Langmuir probe. As the RF power was increased the plasma density increased until the plasma was approximately fully ionized. Additional power increased the electron temperature and plasma potential. Higher mass flow rates provided more neutral gas and thus a higher density when the plasma was fully ionized but also a lower electron temperature and plasma potential.

A linear relationship between the plasma potential and electron temperature as a function of axial position was observed in the experiment, consistent with both the adiabatic theory and rarefaction wave theory. The plasma potential dropped less for a given drop in electron temperature because only the parallel temperature could be measured. The power law relationship between the measured plasma potential and density was consistent with the adiabatic theory with 3 degrees of freedom, suggesting that instabilities may play a crucial role in the dynamics of plasma in a magnetic nozzle. Further experiments are needed to definitively validate the adiabatic theory.

Acknowledgments

Partial support was provided by the University of Houston Institute for Space Systems Operations (ISSO) Postdoctoral Fellowship program for B Longmier, formerly an ISSO Postdoctoral Aerospace Fellow.

References

[1] Longmier B W *et al* 2011 VX-200 magnetoplasma thruster performance results exceeding fifty-percent thruster efficiency *J. Propulsion Power* **27** 915–20
[2] Chen F F and Torreblanca H 2009 Permanent-magnet helicon sources and arrays: a new type of rf plasma *Phys. Plasmas* **16** 057102
[3] Biloiu I A, Scime E E and Biloiu C 2008 Ion beam acceleration in a divergent magnetic field *Appl. Phys. Lett.* **92** 191502
[4] Lafleur T, Charles C and Boswell R W 2011 Characterization of a helicon plasma source in low diverging magnetic fields *J. Phys. D: Appl. Phys.* **44** 055202
[5] Takahashi K, Lafleur T, Charles C, Alexander P and Boswell R W 2011 Electron diamagnetic effect on axial force in an expanding plasma: experiments and theory *Phys. Rev. Lett.* **107** 235001

[6] Wiebold M, Sung Y-T and Scharer J E 2012 Ion acceleration in a helicon source due to the self-bias effect *Phys. Plasmas* **19** 053503
[7] Boswell R W 1984 Very efficient plasma generation by whistler waves near the lower hybrid frequency *Plasma Phys. Control. Fusion* **26** 1147–62
[8] Fruchtman A, Takahashi K, Charles C and Boswell R W 2012 A magnetic nozzle calculation of the force on a plasma *Phys. Plasmas* **19** 033507
[9] Charles C and Boswell R 2003 Current-free double-layer formation in a high-density helicon discharge *Appl. Phys. Lett.* **82** 1356–8
[10] Sutherland O, Charles C, Plihon N and Boswell R W 2005 Experimental evidence of a double layer in a large volume helicon reactor *Phys. Rev. Lett.* **95** 205002
[11] Charles C 2007 A review of recent laboratory double layer experiments *Plasma Sources Sci. Technol.* **16** R1–25
[12] Arefiev A V and Breizman B N 2008 Ambipolar acceleration of ions in a magnetic nozzle *Phys. Plasmas* **15** 042109
[13] Longmier B W *et al* 2011 Ambipolar ion acceleration in an expanding magnetic nozzle *Plasma Sources Sci. Technol.* **20** 015007
[14] Sun X, Cohen S A, Scime E E and Miah M 2005 On-axis parallel ion speeds near mechanical and magnetic apertures in a helicon plasma device *Phys. Plasmas* **12** 103509
[15] Lieberman M A and Charles C 2006 Theory for formation of a low-pressure, current-free double layer *Phys. Rev. Lett.* **97** 045003
[16] Hairapetian G and Stenzel R L 1990 Observation of a stationary, current-free double-layer in a plasma *Phys. Rev. Lett.* **65** 175–8
[17] Ahedo E and Sanchez M M 2009 Theory of a stationary current-free double layer in a collisionless plasma *Phys. Rev. Lett.* **103** 135002
[18] Chen F F 2006 Physical mechanism of current-free double layers *Phys. Plasmas* **13** 034502
[19] Arefiev A V and Breizman B N 2009 Collisionless plasma expansion into vacuum: two new twists on an old problem *Phys. Plasmas* **16** 055707
[20] Arefiev A V and Breizman B N 2005 Magnetohydrodynamic scenario of plasma detachment in a magnetic nozzle *Phys. Plasmas* **12** 043504
[21] Gombosi T I 1998 *Physics of the Space Environment* (Cambridge: Cambridge University Press)
[22] Baalrud S D, Callen J D and Hegna C C 2008 A kinetic equation for unstable plasmas in a finite space-time domain *Phys. Plasmas* **15** 092111
[23] Baalrud S D, Callen J D and Hegna C C 2009 Instability-enhanced collisional effects and Langmuir's paradox *Phys. Rev. Lett.* **102** 245005
[24] Boswell R W *et al* 2004 Experimental evidence of parametric decay processes in the variable specific impulse magnetoplasma rocket (VASIMR) helicon plasma source *Phys. Plasmas* **11** 5125–9
[25] Arefiev A V and Breizman B N 2004 Theoretical components of the VASIMR plasma propulsion concept *Phys. Plasmas* **11** 2942–9
[26] Longmier B W *et al* 2014 Improved efficiency and throttling range of the vx-200 magnetoplasma thruster *J. Propulsion Power* **30** 123–32
[27] Sheridan T E 2000 How big is a small Langmuir probe? *Phys. Plasmas* **7** 3084–8
[28] Hershkowitz N 1989 How Langmuir probes work *Plasma Diagnostics* vol 1 ed O Auciello and D L Flamm (New York: Academic) pp 113–83
[29] Fruchtman A 2008 Neutral depletion in a collisionless plasma *IEEE Trans. Plasma Sci.* **36** 403–13